Alpenglow: Binghamton University Undergraduate Journal of Research and Creative Activity

Volume 1 | Issue 1 Article 7

4-24-2015

Performance Study of a Mems Low-Noise Sound Pressue Gradient Microphone Under an AC Bias

Jonathan Michelson
michel3@binghamton.edu

Abstract
An AC bias was introduced into microelectromechanical system (MEMS) low-noise sound pressure gradient microphone by Miles, Cui, Su and Hormentcovschi (2014), and its implications for the device's noise performance and directivity readings are discussed. The schematic involved demodulation of the microphone output with external circuitry, and subsequent computer software analysis of the microphone and circuitry outputs. Although insights into noise improvement were frustrated due to subpar noisy components used in the demodulation circuitry, the simultaneous measuring of the microphone's varying directivity patterns was shown to be achievable with this AC bias scheme.

Introduction

Miles, Cui, Su and Hormentcovschi (2014), have introduced a novel MEMS microphone with attractive features. It boasts low-noise operation and impressive directivity measurements across a broad frequency range. The diaphragm of the microphone is a fabricated plate hinged to its substrate at a center line. Pressure waves that impinge on its surface cause a rotation back and forth in some combination of two main vibrational modes, depending on the sound source's relative location: about its hinged axis, much like a teeter-totter, or in unison, much like a butterfly's wings. The opposite ends of the plate and diaphragm assembly are lined with interdigitated fingers that form the two lumped capacitive transducers of the microphone. As the plate responds to acoustic pressure gradients, a synchronized varying capacitance is generated and amplified as the electrical microphone output.

The amplification stage necessarily limits the noise performance of the microphone. It is understood that op-amps generally exhibit a phenomenon known as "flicker noise" in which the random distortion imparted to an op-amp's input decreases in magnitude as the frequency of the input signal increases, lending itself the nickname "1/f noise" (Physical Review Letters, 1987). Were the microphone input signal to be amplitude-modulated by a relatively high-frequency AC bias, and then appropriately demodulated at the microphone output, the signal-to-noise ratio of the microphone could be expected to increase by virtue of the "1/f noise" phenomenon. Thus, the

motivation for introducing an AC bias voltage to the capacitive sensors was that similar noise-level improvements might take place.

Additionally, the unique diaphragm schematic of the microphone was suspected to allow for unique multi-directional acoustic sensing. Inherent in the capacitive signal of one end of the hinged plate's motion is the other end's complimentary out-of-phase or in-phase capacitive signal, depending on the sound source's relative location. By combining the two ends' responses, both directional and omnidirectional sound fields could be inferred simultaneously from the microphone's purely physical transduction. Thus the motivation for the introduction of two different AC biases to the two capacitive sensors was clear: encode one diaphragm end's response in one carrier frequency, encode the other end's response in another frequency, and one can simply selectively demodulate the microphone output to obtain corresponding acoustic information about the local environment.

General Experiment Setup

The scheme for Experiment 1, investigation of noise performance with an AC bias present, will be described first. The BK Precision 4055 waveform generator output was T'd, with one end connected to one of the 1.5V battery terminals located in the "bias box" that housed the two 1.5V DC bias terminals, the 9V battery terminal, the DC-to-DC converter for microphone circuitry power, the HDMI output jack through which the microphone "communicated" with this "bias box," and the microphone output BNC jack. From there, an HDMI cable was connected to the HDMI input of a fabricated MEMS microphone labeled "Ckt-8." Ckt-8's unreliable capacitive sensors were replaced by a rough equivalent of two ceramic 0.5pF capacitors, allowing us to bypass Ckt-8's acoustic sensing and focus on its electrical performance. The microphone BNC output was

connected to one input of an Analog Devices AD633 Analog Multiplier chip, while the other end of the waveform generator tee was connected to the other input of the AD633. The AD633's output was fed into the anechoic lab's Brüel & Kjær data acquisition equipment for FFT spectrum analysis in their PULSE platform software. A MATLAB script was used for automating the measurements made with PULSE.

The scheme for Experiment 2, investigation of feasibility of simultaneous directivity measurements, differed only slightly. A fully functional microphone was used in this experiment, after extensive sanity checks that assured little risk when using one. Its identification label was not recorded. A second output of the BK Precision 4055 waveform generator was T'd as well, with one end connected to the second 1.5V battery terminal in the aforementioned "bias box." A second AD633 multiplier was introduced, and the microphone's output BNC jack was T'd and connected to input 1 on both AD633's. Input 2 of the first AD633 received waveform generator output 1, while input 2 of the second AD633 received waveform generator output 2. The multipliers' respective outputs were sent to two separate inputs of the same data acquisition equipment for similar software analysis.

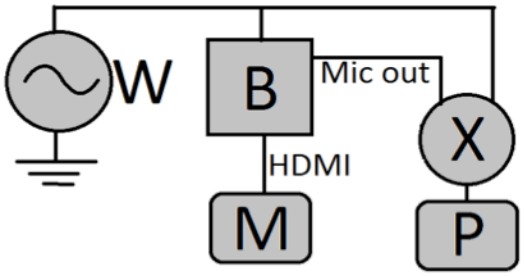

Fig. 1: Block diagram of setup for Experiment 1. Wave generator W, "bias box" B, microphone M, multiplier X, and Pulse hardware P.

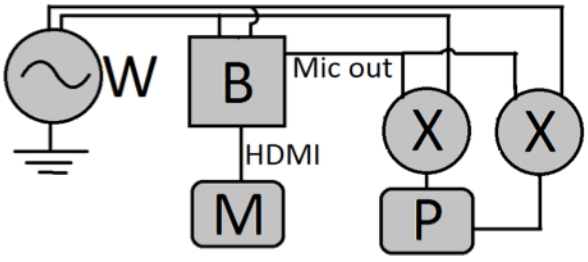

Fig. 2: Block diagram of setup for Experiment 2. Wave generator W, "bias box" B, microphone M, multipliers X, and Pulse hardware P.

Results, Experiment 1

The waveform generator output was set to produce a 10kHz, 2Vpp, 0Vdc offset sine wave. This signal, as described above, was sent to one of the 1.5V terminals in the "bias box" and to one of the inputs of the AD633 multiplier.

Spectral noise of the multiplier output was computed in PULSE. The benchmark against which these results were compared was the voltage noise spectrum response of Miles et al.'s (2014) bare microphone circuit. The multiplier noise spectrum exhibited an impeding noise floor of 1μV/√Hz for frequencies upwards of 2kHz. This phenomenon was consistent with the spectrum noted in the Datasheet for AD633 – Low Cost Analog Multiplier (Analog Devices, 2014). In contrast, Miles et al.'s (2014) bare microphone's noise response logarithmically rolled off at a rate of approximately -3dB per decade, starting with readings of about 20μV/√Hz at 10Hz. Its response crossed the critical 1μV/√Hz level at 1kHz, boasting superior noise performance than the AD633 at frequencies above this marker. Because of this, efforts to gain practical insights into flicker-noise-based improvements were rendered ineffectual. The modulation/demodulation scheme indeed works, but the AD633, being a low-cost device, was too much of a limiting factor for effective implementation.

There is another curious phenomenon worth mentioning that was discovered during the preparation for this experiment. When multiplying two identical 10kHz, 2Vpp, 0Vdc offset sine waves with the AD633, one would expect a prominent peak in the frequency domain only at 20kHz, corresponding to a sinusoid with half the amplitude of its input; the expected multiplication of the two inputs. This follows from the trigonometric identity: 〖sin〗^2 (u) = 1/2-1/2 cos(2u). However, PULSE detected a prominent frequency spike at 10kHz from the AD633 output, suggesting that either: (1) a slight DC artifact from the waveform generator preserved the product

of the 10kHz input with that DC constant at the multiplier output, or (2) the AD633 multiplier internally imparts some DC constant to its inputs, resulting in the preservation of the 10kHz signal as described before. This was investigated extensively to no avail.

Results, Experiment 2

Channel 1 of the waveform generator was set to 200kHz, 1Vpp, 0Vdc offset, and channel 2 was set to 100kHz, 543mVpp, 290mVdc offset. These parameters seemed to encourage the most favorable data – they mitigated suspected DC artifacts, minimized signal distortion to and from the sensitive working microphone, etc. The microphone was placed in the anechoic chamber approximately three meters from speakers that emitted broadband random noise driven from PULSE's signal generator. Per the general experiment setup described earlier, the microphone output was now the summation of both its differentially modulated inputs. This output was T'd and fed into two AD633's, which allowed for separation of the two capacitive sensor's acoustic signals encoded in their respective carrier frequencies.

The microphone was oriented in the chamber with respect to the speakers in such a way that the out-of-phase “teeter-totter” vibrational mode was encouraged. With this setup, nearly identical frequency responses were expected between the two capacitive sensors with a phase shift of π radians between them, to account for the out-of-phase motion inherent in the diaphragm's hinged rocking. Indeed, the phase response of the 100kHz and 200kHz channels differed by approximately 3 radians – nearly π – at their resonant frequency of 650Hz. See Figures 3 and 4 for the corresponding graphical displays. The two channels' noise floors were computed to be 100dBA and 106dBA, respectively—equally unimpressive, yet expected, measurements considering the AD633's performance limitations and the added high frequency activity from the AC biases.

The microphone position was subsequently rotated 90º in the chamber to encourage the in-phase "wing-flapping" vibrational mode. Again, nearly identical frequency responses were expected, this time with little to no phase difference between the channels. However, the obtained phase data was not ideal. The diaphragm was designed to minimize the contribution of this in-phase rocking mode to the overall response, which explains the poor data: this mode occurs at higher frequencies where the coherence of the two channels was measured to be quite poor due to its difficulty to induce. However, the measured magnitude of both channels' frequency responses at the suspected in-phase resonance frequency was approximately 0.2 mV/Pa. This value was found to be in agreement with the magnitude response of the out-of-phase motion at the same frequency, confirming the microphone's omnidirectional capabilities and suggesting its feasible extraction regardless of vibrational mode.

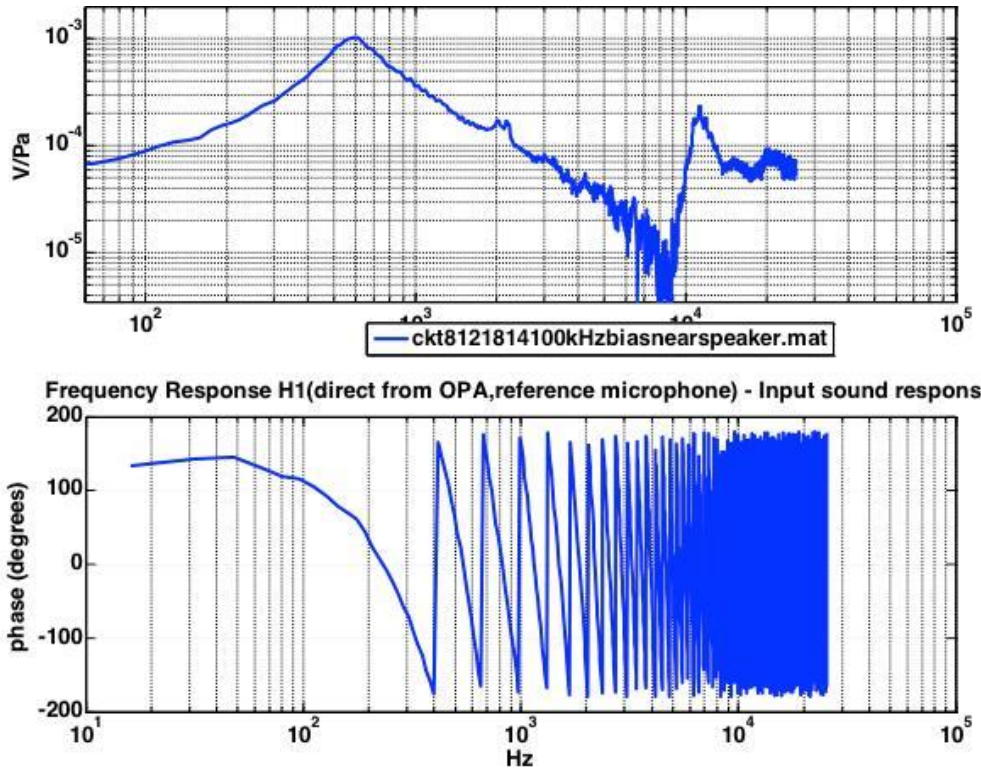

Fig. 3: Frequency response (top) and phase response (bottom) of the 100kHz microphone output channel.

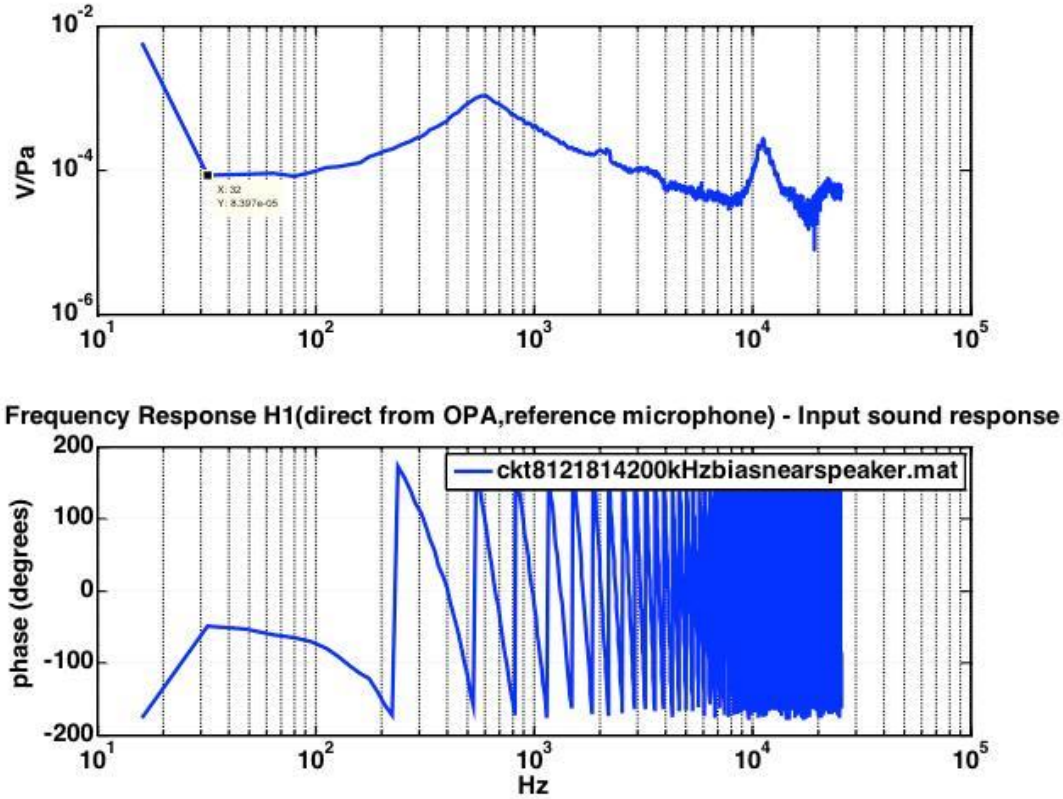

Fig. 4: Frequency response (top) and phase response (bottom) of the 200kHz microphone output channel. Note the approximately 180 degree difference in phase responses of the two channels.

Another microphone position was subjected to testing. It was rotated 45º such that both vibrational modes were equally encouraged. Transfer functions between the two isolated channel outputs were obtained using an edited MATLAB script. The most interesting result was that the sum transfer function of the frequency response eliminated resonance peaks found in the individual channel responses – a result that appears to be consistent with theoretical predictions about off-axis frequency responses in this microphone. Only brief tests were conducted in this orientation. Additional investigation could utilize the anechoic lab's rotation stage setup to obtain frequency response data over an exhaustive sweep of microphone angles.

Conclusions

Experiment 1 confirmed the functionality of the modulation scheme, but ultimately ended inconclusively. The AD633 multiplier used impeded meaningful quantification due to its appreciable noise floor. The most prudent option at this point remains the replacement of the multiplier chip with a higher-quality component.

The results from Experiment 2 show that simultaneous directivity readings are feasible. Despite the frustrating noise floor, the two capacitive sensors' signals were successfully encoded in differing carrier frequencies, combined in the microphone's one output, and extracted via demodulation. Following this verification is the hypothesis that the microphone can depict a more complete picture of the local sound field by isolating the individual channel data. In other words, one can read both vibrational modes simultaneously by measuring to what degree the two channels' responses match each mode. This study urges further comprehensive investigation into this exciting hypothesis.

References

Analog Devices. (2014). Datasheet for AD633 – Low Cost Analog Multiplier. *Analog Devices, Inc. Retrieved from*http://www.analog.com/static/imported-files/data_sheets/AD633.pdf

Bak, P., Tang, C., & Wiesenfeld, K. (1987). Self-organized criticality: an explanation of 1/*f* noise, *Physical Review Letters*, 59, (4), 381–384.

Miles, R., Cui W., Su, Q., & Homentcovschi, D. (2014). A MEMS Low-Noise Sound Pressure Gradient Microphone with Capacitive Sensing. *Journal of Microelectromechanical Systems*, *24, (1),*241-248. doi: 10.1109/JMEMS.2014.2329136